

Novel D3 Selective Dopaminergics Incorporating Enyne Units as Nonaromatic Catechol Bioisosteres: Synthesis, Bioactivity, and Mutagenesis Studies

Miriam Dörfler, Nuska Tschammer, Katharina Hamperl, Harald Hübner, and Peter Gmeiner*

Department of Chemistry and Pharmacy, Emil Fischer Center, Friedrich Alexander University, Schuhstrasse 19, 91052 Erlangen, Germany

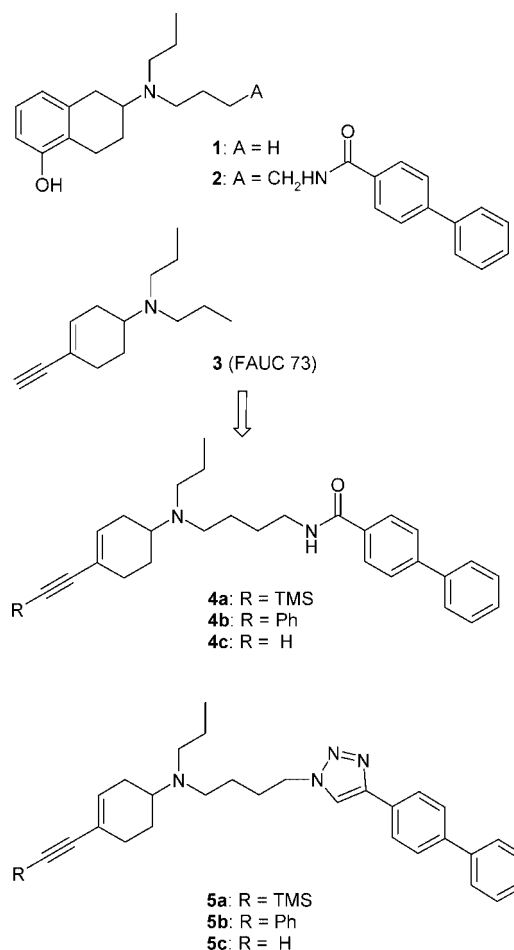
Received July 18, 2008

Enynes of type **4** and **5** as long chain derivatives of the nonaromatic dopamine D₃ receptor agonist **3** (FAUC 73) were prepared by exploiting chemoselective functionalization of the azido-substituted vinyl triflate **9**. Radioligand binding studies indicated excellent D₃ affinity and selectivity over related GPCRs for the terminal alkynes **4c** (FAUC 460) and **5c**. Biphasic displacement curves gave picomolar *K_i* values for the high affinity binding site of D₃. According to mitogenesis experiments and bioluminescence based cAMP assays, the biphenylcarboxamide **4c** and its click chemistry derived triazole analogue **5c** behaved as strong partial agonists but relative ligand efficacy significantly depended on the type of functional assay. Site directed mutagenesis involving the mutants D₃ D3.32E, and D₃ F6.51W implied that ligand interactions with D3.32 and F6.51 are highly crucial, giving rise to analogous binding modes for dopamine, classical and enyne type agonists.

Introduction

The D₂-like dopamine receptors including D₂, D₃, and D₄ have attracted considerable attention since various pharmacological studies have investigated the D₃ system as an interesting therapeutic target for the treatment of schizophrenia, Parkinson's disease, drug-induced dyskinesia, and drug abuse.¹ Moreover, D₃ might be involved in the cortical development orchestrating neuronal migration and differentiation.² Neuroprotective effects during the induction phase of Parkinson's disease have been reported for D₃ receptor agonists. Because of these putative therapeutic applications, D₃ receptor ligands with diverse intrinsic activities have been an active field of research in recent years.^{3,4} Separation of purely D₃-mediated biomolecular activity from effects produced by interactions with similar biogenic amine receptors allows verification of the therapeutic impact of D₃ receptors and to reduce possible side-effects caused by "promiscuous" receptor interactions.⁵ Starting from the endogenous neurotransmitter dopamine, bioisosteric replacement of the catechol function and rigidization of the flexible aminoethyl side chain atoms led to hydroxyl substituted dipropylaminotetralines including 5-HO-DPAT (**1**) and 7-HO-DPAT and heterocyclic analogues thereof as valuable CNS^a drugs and pharmacological tools (Chart 1).⁶ Nevertheless, most dopaminergics are relatively unselective and, in many cases, recognize

Chart 1. Structural Hybridization Leading to the Target Compounds of Type **4** and **5**



* To whom correspondence should be addressed. Phone: +49 9131 85-29383. Fax: +49 9131 85-22585. E-mail: peter.gmeiner@medchem.uni-erlangen.de.

^a Abbreviations: D_x, dopamine D_x receptor; GPCR, G-protein coupled receptor; *K_i*, inhibition constant; cAMP, cyclic adenosine mono phosphate; OH-DPAT, hydroxy-dipropylaminotetralin; CNS, central nervous system; DA, dopamine; THF, tetrahydrofuran; TMS-, trimethylsilyl-; Ph, phenyl; RT, room temperature; CuAAC, copper assisted [3 + 2] azide-alkyne cycloaddition; Ms, methane sulfonyl; Pr, propyl; Chx, cyclohexyl; CHO, Chinese hamster ovary; 5-HT, serotonin; SAR, structure-activity relationship; SEM, standard error of the mean; PKA, protein kinase A; ATP, adenosine triphosphate; EC₅₀, half-maximal effective concentration; PI, phosphoinositol; PKC, protein kinase C; *K_D*, dissociation constant; TM, transmembrane helix; (HR)-EIMS, (high resolution) electron ionization based mass spectroscopy; FT/IR, Fourier transformation/infrared spectroscopy; TFA, trifluoroacetic acid; IC₅₀, half-maximal inhibitory concentration; *n_H*, hill slope; IBMX, isobutyl-1-methylxanthine; Ro 20-1724, 4-(3-butoxy-4-methoxy-benzyl)imidazolidone; cDNA, complementary desoxyribonucleic acid; PCR, polymerase chain reaction; HEK, human embryonic kidney; α-MEM, α-modified Eagle medium; FBS, fetal bovin serum; Pen-Strep, Penicillin–Streptomycin; Eff, efficacy; WT, wild type.

not only the various subtypes of the dopamine receptor but also related monoaminergic GPCRs.⁵

By employing *N*-butyl-4-biphenylcarboxamido substituted phenylpiperazines as lead compounds, previous studies have shown that displacement of one propyl side chain of 5-OH-DPAT by an *N*-butyl-4-biphenylcarboxamido moiety resulted

in D₃ receptor selective structural chimera of type **2** (Chart 1).⁷ By comparing (*S*)-(-)-5-OH-DPAT (**1**) and its long chain carboxamide derivative **2**, not only D₃ affinity ($K_i = 0.20$ nM) but also D₃ selectivity (125-fold) over D₂ could be substantially improved when H-bond accepting substituents in position 5 of the DPAT moiety displayed to be crucial for intrinsic activity.^{7,8}

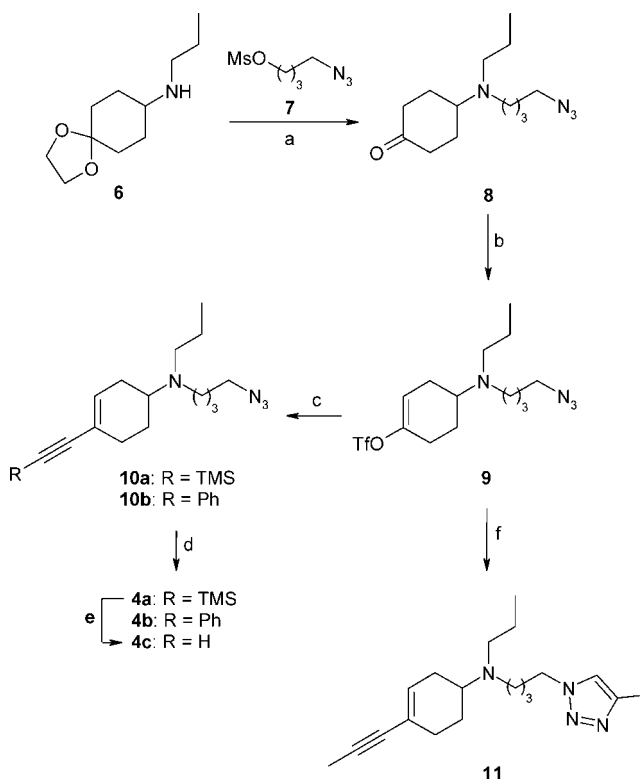
By exploring novel types of arene bioisosteres, we have previously identified nonaromatic dopamine receptor agonists when conjugated enyne systems proved to be able to simulate the catechol substructure of dopamine.^{9–12} In fact, the terminal enyne FAUC 73 (**3**, Chart 1) was found to be a subtype selective D₃ agonist when the high D₂/D₃ discrimination ratio obviously originates from a significant reduction of D₂ affinity.⁹ Although the nonaromatic conjugated system of **3** revealed a more lipophilic and less polar character than the catechol ring of DA, a computational study corroborated our assumption that the conjugated enyne functionality shows molecular properties that are similar to those of the catechol subunit of DA. Particularly at the D₃ receptor, the ability of the more lipophilic enyne system to facilitate hydrophobic interactions seems to compensate for slightly reduced attractive forces resulting from electrostatic interactions.

To design highly potent and selective D₃ agonists, we envisaged to formally ligate key molecular scaffolds of both lead compounds **2** and **3**, resulting in novel hybrids of type **4**. Taking advantage of previous studies indicating that the carboxamide function of related D₃ antagonists can be successfully replaced by five-membered heteroarenes,^{13–17} 1,2,3-triazole analogues of type **5** should be approached via click chemistry.^{18–20} In this paper, we describe chemical synthesis, receptor binding studies, and functional assays of the target compounds **4** and **5**. To investigate if our enyne derived bioisosteres **3**, **4**, and **5** adopt a binding mode that is analogous to the neurotransmitter dopamine and classical dopamine receptor agonists, site directed mutagenesis experiments and the investigation of truncated test compounds have been performed.

Results and Discussions

Synthesis. Our plan of synthesis depended on a chemoselective functionalization of the azido-substituted vinyl triflate **9** (Scheme 1). Choosing this key intermediate, we should be able to realize in a consecutive and orthogonal way palladium-catalyzed C–C bond formation for the construction of the enyne moiety and the synthesis of the carboxamide moiety via Staudinger-type reduction and *N*-acylation. As a starting compound, we used the acetal-protected aminocyclohexanone **6**, which was readily prepared by reductive amination of 1,4-cyclohexanedione monoethylene acetal.²¹ Nucleophilic substitution with 4-azidobutanol methane sulfonate **7**²² and subsequent hydrolysis of the acetal substructure afforded the cyclohexanone **8**, which was transformed into the vinyl triflate **9** by *O*-sulfonylation. Transition metal-catalyzed reaction of the vinyl triflate **9** was performed following a protocol described by Cacchi using a reaction mixture of PdCl₂(PPh₃)₂, CuI, EtMe₂N, and THF. Thus, the conjugated enyne **10a** could be readily accessed employing TMS-acetylene. It is noteworthy that the stoichiometry had to be carefully tuned to selectively accomplish C–C coupling without any copper assisted [3 + 2] azide-alkyne cycloaddition (CuAAC) as a side reaction. When we utilized an excess of gaseous propyne, transition metal promoted reaction of the vinyl triflate **9** resulted in formation of the triazolyl substituted enyne **11**. Staudinger reduction of the azide **10a** and subsequent *N*-acylation of the intermediately formed primary

Scheme 1^a

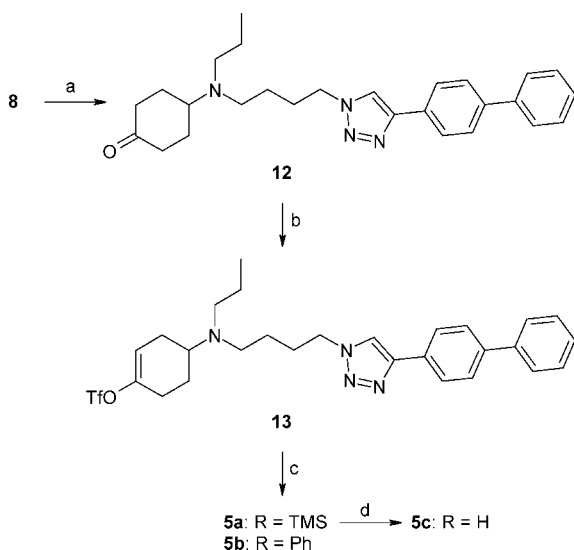


^a Reagents and conditions: (a) **7**, K₂CO₃, NaI, CH₃CN, reflux, 3 d; (2) 6 N HCl, acetone, RT, 19.5 h. (b) Tf₂O, 2,6-di-*tert*-butyl-4-methylpyridine, 1,2-dichloroethane, reflux, 4.5 h. (c) RC≡CH, CuI, PdCl₂(PPh₃)₂, EtMe₂N, THF, RT, 35–40 min. (d) (1) PPh₃, THF, H₂O, RT, 2 d; (2) 4-biphenylcarboxylic acid chloride, Et₃N, CHCl₃, RT, 3/24 h. (e) Bu₄NF, THF, –15 °C, 165 min. (f) Propyne (–45 °C to rt), CuI, Pd Cl₂(PPh₃)₂, piperidine, THF, RT, 2 h.

amines with 4-biphenylcarboxylic acid chloride furnished the target compound **4a**. Cleavage of the trimethylsilyl group with Bu₄NF gave access to the terminal enyne **4c**. Pd-promoted coupling of the intermediate **9** with phenylacetylene led to **10b** and hardly separable side products. Thus, crude **10b** was subjected to Staudinger conditions and transformed into the final product **4b**, resulting in low overall yield (4%). Taking advantage of click chemistry, the synthesis of the triazole based carboxamide isosteres **5a–c** was performed via copper(I)-promoted [3 + 2] azide-alkyne cycloaddition (CuAAC). Thus, the azido substituted intermediate **8** was reacted with 4-biphenylacetylene in the presence of [Cu(CH₃CN)₄]PF₆ (Scheme 2). In fact, complete regiocontrol was observed, resulting in formation of the 1,4-substituted biphenyltriazole **12** in 76% yield. *O*-Activation by treatment with triflic anhydride afforded the vinyl sulfonate **13**, which could be transformed into the enyne derivatives **5a,b** via Pd/Cu-catalyzed cross coupling reaction. Fluoride promoted desilylation of the TMS-protected enyne **5a** yielded the final product **5c**.

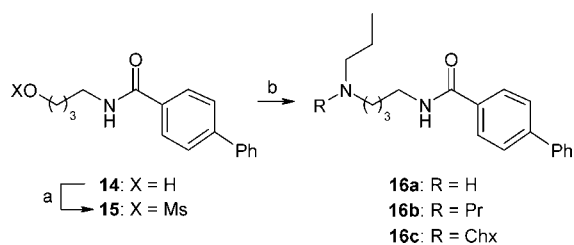
To investigate the importance of the butenyn substructure as a primary pharmacophoric element, truncated test compounds of type **16a–c** were prepared (Scheme 3) starting from *N*-(4-hydroxybutyl)-4-biphenylcarboxamide²³ (**14**). Activation of the primary alcohol function gave the methane sulfonate **15**, which was subjected to nucleophilic displacement reactions to afford the secondary amine **16a** and the dipropylamine derivative **16b**. The cyclohexyl substituted test compound **16c** was prepared via *N*-alkylation and reductive alkylation.

Receptor Binding. Radioligand binding assays were employed to analyze affinity and selectivity profiles of the target

Scheme 2^a

^a Reagents and conditions: (a) 4-biphenylacetylene, [Cu(CH₃CN)₄]PF₆, CH₂Cl₂/MeOH 3:1, 40 °C, 25 h. (b) Tf₂O, 2,6-di-*tert*-butyl-4-methylpyridine, 1,2-dichloroethane, reflux, 15 h. (c) R-C≡CH, CuI, PdCl₂(PPh₃)₂, EtMe₂N, THF, RT, 90 min; (d) Bu₄NF, THF, -15 °C, 150 min.

Scheme 3.



^a Reagents and conditions: (a) MsCl, Et₃N, THF, RT, 2.5 h. (b) **16a**: *n*-PrNH₂, NaI, K₂CO₃, CH₃CN, reflux, 6 h; **16b**: Pr₂NH, NaI, K₂CO₃, CH₃CN, reflux, 16 h; **16c**: (1) ChxNH₂, NaI, K₂CO₃, CH₃CN, reflux, 14 h; (2) propionaldehyde, NaBH(OAc)₃, CH₂Cl₂, RT, 7 h.

compounds. The binding data was generated by measuring their ability to compete with [³H]spiperone for the cloned human dopamine receptor subtypes D_{2long}, D_{2short},²⁴ D₃,²⁵ and D_{4.4}.²⁶ stably expressed in Chinese hamster ovary cells (CHO). D₁ receptor affinities were determined utilizing porcine striatal membranes and the D₁ selective radioligand [³H]SCH 23390. The ligands were also investigated for their potency to displace [³H]WAY100635, [³H]ketanserin, and [³H]prazosin when employing porcine 5-HT_{1A}, 5-HT₂, and α₁ receptors, respectively. Compared to the neurotransmitter dopamine, the resulting K_i values are listed in Tables 1 and 2.

Our initial studies involved the evaluation of binding affinities for the dopamine D₃ receptor as our primary target protein. In agreement with our recent SAR data on dipropylamine substituted enyne derivatives, the phenylalkynes **4b** and **5b** displayed only moderate receptor recognition. On the other hand, K_i values in the low nanomolar range were observed for the trimethylsilyl analogues **4a** and **5a** (K_i = 4.4 nM and 13 nM, respectively). Excellent D₃ affinity was found for terminal alkynes when a subnanomolar K_i for the carboxamide **4c** (0.21 nM), which is comparable to the reference data for **2** (K_i = 0.20 nM),⁷ and a K_i of 1.3 nM for its triazole derived congener **5c** indicated that a molecular appendage formally ligated to one of the *N*-propyl groups is highly beneficial for D₃ binding of both classical dopaminergics and atypical bioisosteres. Poor D₃ recognition of the truncated analogues **16a–c** renouncing the enyne moiety

Table 1. Receptor Binding Data for Dopamine, **4a–c**, **5a–c**, **11**, and **16a–c** Employing Human D_{2long}, D_{2short}, D₃, and D_{4.4} Receptors

compd	R	K _i /K _{0.5} Values (nM) ± SEM ^a			
		[³ H]spiperone			
		hD _{2long}	hD _{2short}	hD ₃	hD ₄
dopamine		450 ± 90	360 ± 16	240 ± 31	6.2 ± 1.4
4a	TMS	220 ± 62	360 ± 71	4.4 ± 0.84	69 ± 15
4b	Ph	5500 ± 1100	4700 ± 1500	300 ± 32	3100 ± 140
4c	H	40 ± 4.7	43 ± 4.7	0.21 ± 0.030	4.3 ± 0.51
5a	TMS	690 ± 86	670 ± 230	13 ± 1.2	1800 ± 220
5b	Ph	210 ± 57	180 ± 52	150 ± 37	1100 ± 160
5c	H	610 ± 170	170 ± 23	1.3 ± 0.22	190 ± 91
11		4100 ± 450	2100 ± 710	280 ± 27	100 ± 19
16a	H	21000 ± 7800	>100000	11000 ± 1 00	6100 ± 210
16b	<i>n</i> -Pr	9700 ± 2300	8800 ± 850	950 ± 460	1400 ± 410
16c	<i>cy</i> -Hex	4700 ± 570	6300 ± 3 400	140 ± 3.5	670 ± 140

^a Derived from 2–18 experiments, each done in triplicate.

Table 2. Receptor Binding Data for Dopamine, **4a–c**, **5a–c**, **11**, and **16a–c** Employing Porcine D₁, 5-HT_{1A}, 5-HT₂, and α₁ Receptors

compd	R	K _i /K _{0.5} Values (nM) ± SEM ^a			
		[³ H] SCH23390	[³ H] WAY100635	[³ H] ketanserin	[³ H] prazosin
		pD ₁	p5-HT _{1A}	p5-HT ₂	pα ₁
dopamine					
4a	TMS	3800 ± 410	660 ± 57	1400 ± 180	2200 ± 310
4b	Ph	13000 ± 3400	5800 ± 1300	8300 ± 350	4600 ± 280
4c	H	2900 ± 35	230 ± 42	460 ± 42	510 ± 11
5a	TMS	5800 ± 280	6900 ± 2900	8300 ± 280	1900 ± 350
5b	Ph	1700 ± 280	5900 ± 670	5700 ± 780	900 ± 74
5c	H	9500 ± 3 900	2500 ± 350	2700 ± 1100	4400 ± 1500
11		>100000	1800 ± 280	15000 ± 4700	8700 ± 1400
16a	H	7300 ± 1 500	9500 ± 390	860 ± 240	2500 ± 180
16b	<i>n</i> -Pr	6800 ± 490	2800 ± 460	790 ± 110	2400 ± 460
16c	<i>cy</i> -Hex	4600 ± 210	1200 ± 110	890 ± 67	1100 ± 35

^a Derived from 2–18 experiments, each done in triplicate.

(K_i = 140–11 000 nM) clearly reveals that the conjugated π-system is of primary importance for the dopaminergic pharmacophore obviously adopting the catechol ring. As observed for the lead compound **3**,^{9–12} the test compounds of type **4** and **5** as well as the methyltriazole **11** and the truncated analogues **16a–c** showed only weak to modest affinity for the D₁, D_{2long}, D_{2short}, 5-HT_{1A}, 5-HT₂, and α₁ receptors. Except for **4c** (K_i = 4.3 nM), the test compounds were also devoid of substantial D₄ affinity. As a consequence, **4a,c** and **5a,c** display extraordinary D₃ selectivity over related GPCRs when the most potent test compound **4c** (FAUC 460) gave selectivity ratios over D₁, D_{2long}, D_{2short}, 5-HT_{1A}, 5-HT₂, and α₁ between 200 and >10000 and 20 over D₄. The overall D₃ selectivity of the triazole analogue **5c** displaying only moderate D₄ affinity was between 130 and >7000. Thus, replacement of the carboxamide motif by a triazole moiety led to a minor loss of D₃ affinity and a significant increase of selectivity over D₄.

For dopamine D₃ receptor agonists, biphasic displacement curves were reported, indicating a two-site model.^{9–12,27} Careful analysis of the D₃ binding investigations employing a large number of test concentrations and repeating experiments displayed biphasic displacement curves for the most promising test compounds **4c** and **5c**, when the respective Hill coefficients and a better fit of equations indicated a two-site competition with **14** and **12** as well as 86 and 88% population for the high and low affinity binding sites, respectively (Table 3). Thus, K_i values of 0.011 and 0.11 nM for the high affinity binding sites representing the G-protein coupled ternary complexes could be determined for the carboxamide **4c** and the triazole **5c**, respectively. By comparing these data to the K_i high value of 5.2 nM for the lead compound **3**, our concept of structural

Table 3. D₃ Receptor Binding Data for **3**, **4c**, and **5c** Calculated in a Two-Site Model and Their Intrinsic Activities Determined by Measuring the Stimulation of Mitogenesis^a and the Decrease of cAMP Concentration^b in Comparison to the Reference Quinpirole

compd	binding: two-site model ^c		mitogenesis		cAMP assay	
	K _i high	K _i low	EC ₅₀ ^g	eff ^h	EC ₅₀ ⁱ	eff ^h
3	5.2 ^d	590	4.4	74	7.7	101
4c	0.011 ^e	0.28	1.6	72	2.1	36
5c	0.11 ^f	1.4	2.6	64	3.1	40
quinpirole			2.1	100	2.9	100

^a Incorporation of [³H]thymidine in CHO dhfr[−] cells expressing the human D₃ receptor. ^b Bioluminescence based cAMP-Glo assay from Promega using a hD₃ expressing CHO dhfr[−] cell line. ^c Derived from detailed analysis of the binding data using a nonlinear algorithm to describe a biphasic binding mode. ^d Hill slope: −0.60; population 23%. ^e Hill slope: −0.83; population 14%. ^f Hill slope: −0.89; population 12%. ^g EC₅₀ values in [nM] derived from the mean curves of 6–10 experiments each done in hexaduplicate. ^h Ligand efficacy in [%] compared to the full agonist quinpirole. ⁱ EC₅₀ values in [nM] derived from the mean curves of five experiments, each done in duplicate.

hybridization was displayed to be very fruitful when the exchange of a *N*-propyl side chain by carboxamide and triazole based *long chain analogues* led to substantial increase of affinity.

Functional Experiments. To investigate the intrinsic effects of the terminal enynes **4c** and **5c** compared to the full agonist quinpirole, a mitogenesis assay was performed by employing CHO dhfr[−] cells expressing a human D₃ receptor²⁵ as well as a bioluminescence based cAMP assay. In case of the mitogenesis assay, agonist activation of dopamine receptors can be determined by measuring the rate of [³H]thymidine incorporation into growing heterologously transfected cell lines. In the bioluminescence based cAMP assay, the activation of cAMP-dependent protein kinase (PKA) is monitored by measuring ATP utilization in a kinase reaction by using a luciferase/luciferin luminescent reaction.²⁸ After initial stimulation of the adenylyl cyclase with forskolin, the enzyme is dose-dependently inhibited upon D₃ receptor activation. Thus, reduced cAMP production is measured as an increase of luminescence.

Intrinsic activities and EC₅₀ values are depicted in Table 3, indicating high partial agonist properties for **3**, **4c**, and **5c** with 74%, 72%, and 64%, respectively, in the case of the mitogenesis assay with slightly declined EC₅₀ values compared to the K_i values (Figure 1, above). The cAMP assay displays lower efficacy for **4c** (36%) and **5c** (40%), whereas **3** turned out to be a full agonist (Figure 1, below). The EC₅₀ values determined for the enynes **4c** (2.1 nM) and **5c** (3.1 nM) strongly resemble their EC₅₀ values of the mitogenesis experiment (1.6 nM and 2.6 nM, respectively).

For the selected test compounds **3**, **4c**, and **5c**, the differences in the efficacy between the two functional assays employed may be interpreted as a result of functional selectivity.^{29–31} It is hypothesized that the functional selectivity may be a result of ligand-specific induced conformation of GPCR receptors that results in an activation of only selected signaling pathways. Additionally, new evidence arose that D₃ receptors appears to initiate additional signaling events that are not G_i/G_o protein-mediated.³² The pertussis toxin and wortmannin independent phosphorylation of the β-subunit of elongation factor-1B was observed in the response of the stimulation of D₃ receptor, indicating the lack of involvement of G_i/G_o or the PI-cascade.³³ This signaling event appeared to be dependent on PKC activity, thus linking G_i/G_o-independent D₃ signaling with the regulation of protein synthesis or cell proliferation.

Mutagenesis. Site-directed mutagenesis was employed to determine crucial residues within the binding pocket of the D₃

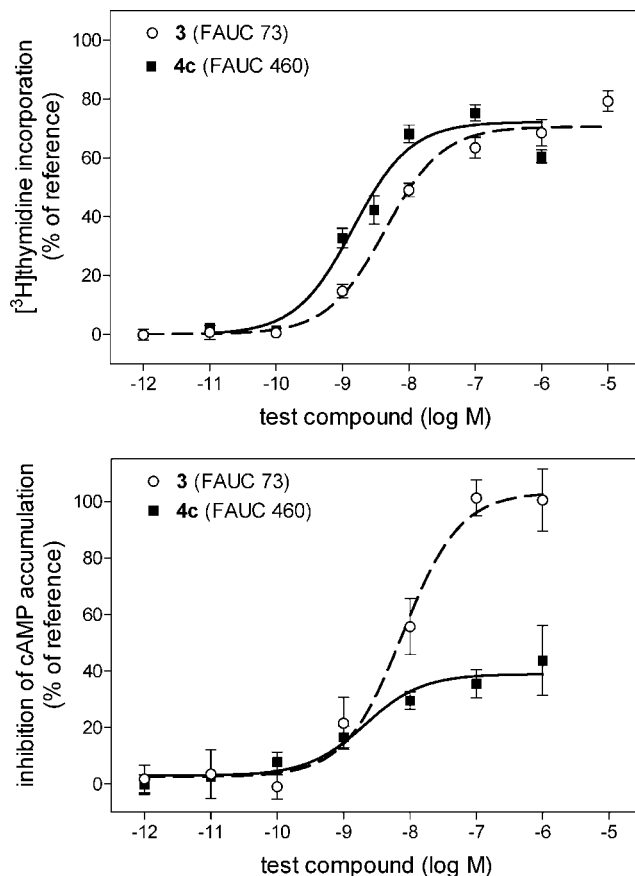


Figure 1. Functional activity of test compound **4c** compared to **3** employing mitogenesis experiments (above) and cAMP assays (below).

receptor that interact with our substances. The binding site crevice of dopamine receptors is thought to be determined by several highly conserved amino acids, among which D3.32 and F6.51 seem to be of crucial importance.^{34–36} Whereas D3.32 is accepted as a key residue displaying a reinforced H-bond³⁷ with the protonated amino function of the ligand, F6.51 is a crucial element of an aromatic cluster³⁶ interacting with the catechol ring of dopamine or a respective arene bioisostere of dopamine agonists. To corroborate our previous SAR analyses indicating that the enyne function acts as a surrogate for the catechol unit, mutagenesis studies were envisaged when analogous susceptibilities were expected for dopamine, classical dopaminergics, and our enyne based representatives. To inspect the binding mode of **3**, **4c**, and **5c**, we initially mutated D3.32 and F6.51 into the serine and alanine mutants D₃ D3.32S and D₃ F6.51A, respectively. The mutants D₃ D3.32S and D₃ F6.51A showed no detectable binding of [³H]spiperone and [³H]7-OH-DPAT. Following the guidelines for “safe” amino acids substitutions, which are least likely to disturb the protein structure, either locally or in its overall folding pathway, and most likely to allow probing of the structural and functional significance of the substituted site,³⁸ we substituted aspartate with glutamate (mutant D₃ D3.32E) and phenylalanine with tryptophane (mutant D₃ F6.51W). This substitutions yielded mutants that were able to bind [³H]spiperone. The K_D values were 0.52, 1.85, and 0.23 nM for the D₃ wild type, D₃ D3.32E, and D₃ F6.51W receptors, respectively. The affinities of the mutants D₃ D3.32E and D₃ F6.51W for dopamine, 7-OH-DPAT, **3**, **4c**, and **5c** were notably influenced. The mutation of aspartate 3.32 to glutamate caused significant reduction in the binding affinities of 7-OH-DPAT, compounds **4c** and **5c** (for factor 390,

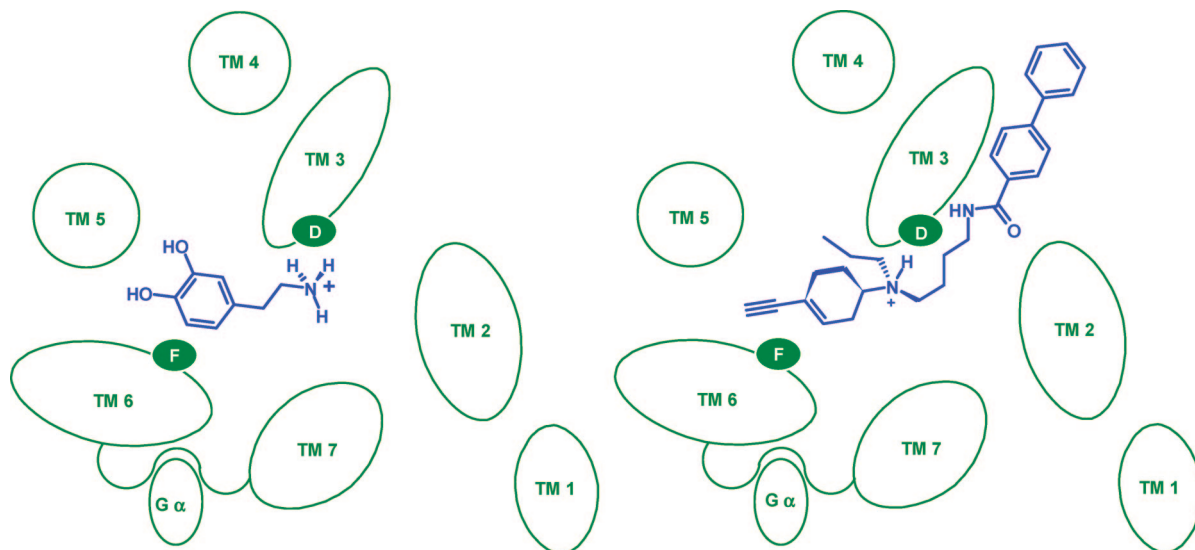


Figure 2. Conceptual model of the binding mode of dopamine (left) and compound **4c** (right).

Table 4. Receptor Binding Data for Dopamine, 7-OH-DPAT, **3**, **4c**, and **5c** Employing Human D₃ Wild Type, D₃ D3.32E, and D₃ F6.51W Receptors, Transiently Expressed in HEK 293 Cells; K_i Values (nM) as Mean of 2–6 Experiments ± SEM

compd	D ₃ WT	D ₃ D3.32E		D ₃ F6.51W	
	K _i	K _i	K _i (D3.32E)/ K _i (WT)	K _i	K _i (F6.51W)/ K _i (WT)
dopamine	72 ± 17	1 100 ± 140	15	>80000	>1100
7-OH-DPAT	3.6 ± 1.5	1 400 ± 210	390	270 ± 40	74
3	190 ± 80	>10 000	>53	5700 ± 1900	30
4c	0.78 ± 0.21	870 ± 180	1100	20 ± 0.7	25
5c	2.5 ± 0.81	1500 ± 290	610	33 ± 10	13

1100, and 610, respectively). Compound **3** showed no detectable binding (Table 4).

The mutant D₃ F6.51W had moderately altered affinities for 7-OH-DPAT, **3**, **4c**, and **5c** (factor 74, 30, 25, and 13, respectively). This implies that the investigated enynes **3**, **4c**, and **5c** most likely have a similar binding mode as 7-OH-DPAT and depend on the interaction with D3.32 and F6.51. For dopamine, both mutations caused also a significant reduction of affinity, indicating an analogous binding mode. When compared to our dopamine agonists displaying 50–1100 and 13–74-fold loss of affinity for the D3.32E and the F6.51W mutation, respectively, significantly weaker (15-fold) and stronger (>1100-fold) susceptibilities show that the energetic contributions of both positions for dopamine are different. Because ligand–receptor interactions of dopamine will be dominated by the catechol moiety facilitating π -interactions toward the aromatic cluster of TM 6 and H-bond interactions with serine residues in TM 5 (S5.42, S5.43, S5.46), perturbation by the exchange of Phe into the sterically demanding Trp leads to a dramatic loss of affinity. Interactions of the primary amine function located on a conformationally nonrestricted ethyl residue will be less influenced by the D3.32E exchange, as this more flexible ethyl side chain may be able to compensate for the altered distance of the primary amine to the carboxylate group of the target protein. Because the primary nitrogen atom is devoid of alkyl substituents, the loss of affinity will be weaker than for the tertiary amines 7-OH-DPAT, **3**, **4c**, and **5c**. Microcalorimetric experiments could be useful to determine the entropic or enthalpic contributions to the binding constants of ligands at the wild type and the mutated receptor.³⁹ A conceptual model

of the complex between D₃ and dopamine (left) and the enyne **4c** (right) is displayed in Figure 2.

Conclusion

Enynes of type **4** and **5** as long chain derivatives of the recently described nonaromatic dopamine surrogate **3** were approached via a five-step synthesis. Radioligand binding studies indicated excellent D₃ affinities for the terminal alkynes as well as an extraordinary selectivity over related GPCRs. Biphasic displacement curves gave picomolar K_i values for the high affinity binding sites of the terminal alkynes **4c** and **5c**, respectively. Thus, our concept of structural hybridization was displayed to be very fruitful when the exchange of a *N*-propyl side chain by carboxamide and triazole based *long chain analogues* led to substantial increase of affinity. Because only poor D₃ recognition was determined for the truncated analogues **16a–c**, the conjugated π -system is of primary importance for the dopaminergic pharmacophore obviously adopting the catechol ring. Employing mitogenesis experiments, **3**, **4c**, and **5c** showed high partial agonist properties (74%, 72%, and 64%, respectively), whereas a cAMP assay displayed reduced efficacy for the long chain analogues **4c** (36%) and **5c** (40%) compared to a full agonism of the dipropylamine **3**. Site directed mutagenesis experiments were performed following the guidelines for “safe” amino acids substitutions when the affinities of the mutants D₃ D3.32E and D₃ F6.51W for 7-OH-DPAT, **3**, **4c**, and **5c** were clearly influenced. This implies D₃ receptor binding depended on the interaction with D3.32 and F6.51,

giving rise to a similar binding mode as dopamine and classical dopamine receptor agonists.

Experimental Section

Chemistry. All reactions were carried out under nitrogen atmosphere. Dry solvents and reagents were of commercial quality and were used as purchased. MS were run on a Finnigan MAT TSQ 700 spectrometer by EI (70 eV) with solid inlet. NMR spectra were obtained on a Bruker Avance 360 or a Bruker Avance 600 spectrometer relative to TMS in the solvents indicated (*J* value in Hz). IR spectra were performed on a Jasco FT/IR 410 spectrometer. Purification by flash chromatography was performed using Silica Gel 60 if not stated otherwise; TLC analyses were performed using Merck 60 F254 aluminum sheets and analyzed by UV light (254 nm) in the presence of iodine or by spraying with ninhydrin reagent. Preparative and analytical HPLC was performed on Agilent 1100 HPLC systems employing a VWL detector. CHN elementary analyses were performed at the chair of Organic Chemistry of the Friedrich Alexander University Erlangen–Nürnberg or at Beetz, Mirkroanalytisches Laboratorium Kronach (compounds **3a**, **3c**).

***N*-[*N*'-Propyl-*N*'-[4-(2-trimethylsilylethynyl)cyclohex-3-en-1-yl]-4-aminobutyl]-4-biphenylcarboxamide (**4a**).** A solution of **10a** (32.5 mg, 0.10 mmol) in THF (4 mL) was added to PPh₃ (130.7 mg, 0.50 mmol). After addition of H₂O (1 mL), the mixture was stirred at room temperature for 2 d. Then, the mixture was diluted with Et₂O (100 mL), dried (Na₂SO₄), and evaporated. After dissolving the residue in CHCl₃ (5 mL), Et₃N (0.05 mL, 0.36 mmol) was added and the mixture was cooled to 0 °C. Then, a solution of 4-biphenyl carboxylic acid chloride (92.1 mg, 0.43 mmol) in CHCl₃ (5 mL) was added dropwise and the mixture was allowed to warm to room temperature. After being stirred at this temperature for 3 h, saturated aqueous NaHCO₃ was added and the aqueous layer was extracted with CH₂Cl₂. The combined organic layers were dried (Na₂SO₄) and evaporated. The residue was purified by flash chromatography (CH₂Cl₂–MeOH 98:2 and hexane–EtOAc 4:1 + 0.5% NMe₂Et) to give **4a** as a colorless oil (15.8 mg, 33% yield). IR: 3352, 2954, 2631, 2866, 2141, 1635, 1547, 1435, 1250, 1130, 1003, 841 cm⁻¹. ¹H NMR (600 MHz, CDCl₃) δ 0.17 (s, 9 H), 0.85 (t, 3 H, *J* = 7.3 Hz), 1.38–1.49 (m, 3 H), 1.53 (m, 2 H), 1.66 (m, 2 H), 1.83 (m, 1 H), 2.02–2.10 (m, 1 H), 2.15–2.30 (m, 3 H), 2.39 (m, 2 H), 2.49 (m, 2 H), 2.77 (m, 1 H), 3.48 (m, 2 H), 6.12 (m, 1 H), 6.43 (m, 1 H), 7.39 (m, 1 H), 7.46 (m, 2 H), 7.60–7.67 (m, 4 H), 7.83 (m, 2 H). ¹³C NMR (150 MHz, CDCl₃) δ 0.03, 11.83, 21.61, 24.87, 26.08, 27.44, 28.02, 30.13, 39.86, 50.00, 52.46, 55.68, 91.80, 106.27, 120.67, 127.18, 127.19, 127.43, 127.91, 128.88, 133.49, 135.30, 140.10, 144.12, 167.29. EIMS *m/z* 487. Anal. (C₃₁H₄₂N₂O₂Si) C, H, N.

***N*-[*N*'-Propyl-*N*'-[4-(2-phenylethynyl)cyclohex-3-en-1-yl]-4-aminobutyl]-4-biphenylcarboxamide (**4b**).** Compound **4b** was prepared according to the protocol of **4a** using crude **10b** (37 mg, approximately 0.11 mmol) in THF (4 mL), PPh₃ (154.8 mg, 0.59 mmol), and H₂O (1 mL).

For the acylation, CHCl₃ (5 mL), Et₃N (0.06 mL, 0.43 mmol), and a solution of 4-biphenyl carboxylic acid chloride (125.0 mg, 0.58 mmol) in CHCl₃ (5 mL) were used. Stirring at room temperature for 24 h, workup according to **4a** and purification by HPLC (CH₃CN–H₂O + 0.1% TFA, gradient) yielded **4b** as a white solid (TFA salt, 2.6 mg, 4% yield (referring to **9** as starting material)). IR: 3745, 3645, 3531, 3126, 2779, 2738, 2434, 2306, 2214, 1647, 1612, 1574, 1558, 1390, 1138, 1078 cm⁻¹. ¹H NMR (360 MHz, CD₃OD, TFA salt) δ 1.04 (t, 3 H, *J* = 7.4 Hz), 1.71–1.96 (m, 7 H), 2.19 (m, 1 H), 2.44–2.66 (m, 4 H), 3.04–3.28 (m, 4 H), 3.51 (m, 2 H), 3.63 (m, 1 H), 6.09 (m, 1 H), 7.29–7.41 (m, 6 H), 7.45 (m, 2 H), 7.46–7.45 (m, 4 H), 7.92 (m, 2 H). ¹³C NMR (90 MHz, CD₃OD, TFA salt) δ 11.24, 19.49, 19.69, 23.08, 23.26, 24.15, 24.24, 27.04, 27.15, 27.75, 29.91, 39.46, 51.77, 52.09, 53.61, 53.94, 60.42, 89.54, 89.64, 122.28, 124.27, 128.02, 128.05, 128.75, 129.05, 129.31, 129.39, 129.93, 130.32, 132.31, 133.92, 141.05, 145.79, 170.04. HR-EIMS *m/z* 490.2984; purity HPLC.

***N*-[*N*'-(4-Ethynylcyclohex-3-en-1-yl)-*N*'-propyl-4-aminobutyl]-4-biphenylcarboxamide (**4c**).** To a solution of **4a** (23.9 mg; 0.05 mmol) in THF (5 mL), a 1 molar solution of tetrabutylammoniumfluoride (0.1 mL, 0.1 mmol) was added at –15 °C. After being stirred at this temperature for 165 min, saturated aqueous NaHCO₃ was added and the mixture was allowed to warm to room temperature. The aqueous layer was extracted with CH₂Cl₂, and the combined organic layers were dried (MgSO₄) and evaporated. The residue was purified by flash chromatography (CH₂Cl₂–MeOH 98:2) to give **4c** as a colorless oil (13.2 mg, 65% yield). IR: 3491, 3352, 1655, 1427, 1346, 1257, 1130, 999, 945, 825 cm⁻¹. ¹H NMR (360 MHz, CDCl₃) δ 0.87 (t, 3 H, *J* = 7.3 Hz), 1.41–1.73 (m, 7 H), 1.90 (m, 1 H), 2.04–2.34 (m, 4 H), 2.46 (m, 2 H), 2.56 (m, 2 H), 2.79–2.91 (m, 2 H), 3.49 (m, 2 H), 6.11–6.16 (m, 1 H), 6.56 (m, 1 H), 7.35–7.50 (m, 3 H), 7.58–7.68 (m, 4 H), 7.85 (m, 2 H). ¹³C (90 MHz, CDCl₃) δ 11.82, 21.56, 24.79, 25.96, 27.44, 27.99, 30.03, 39.84, 50.03, 52.46, 55.67, 75.06, 84.78, 119.72, 127.17, 127.19, 127.43, 127.92, 128.88, 133.49, 135.05, 140.08, 144.13, 167.29. EIMS *m/z* 414. Anal. (C₂₈H₃₄N₂O) C, H, N.

***N*-[4-[4-(4-Biphenyl)triazol-1-yl]butyl]-*N*-propyl-*N*-[4-(2-trimethylsilylethynyl)cyclohex-3-en-1-yl]amine (**5a**).** Compound **5a** was prepared according to **10a** using a solution of **13** (17.6 mg, 0.03 mmol) in THF (5 mL), Cu(I)I (10.4 mg, 0.05 mmol) and Pd(PPh₃)₂Cl₂ (17.1 mg, 0.02 mmol) as well as NMe₂Et (0.05 mL, 0.46 mmol) and TMS-acetylene (15 μL, 0.11 mmol). Stirring at room temperature for 90 min, workup according to **10a**, and purification by flash chromatography (CH₂Cl₂–MeOH 98:2 and hexane–EtOAc 4:1 + 0.5% NMe₂Et) yielded **5a** as a yellow solid (6.6 mg, 41% yield). IR: 3766, 2841, 2646, 1676, 1583, 1502, 1412, 1030, 818 cm⁻¹. ¹H NMR (360 MHz, CDCl₃) δ 0.17 (s, 9 H), 0.85 (t, 3 H, *J* = 7.3 Hz), 1.33–1.53 (m, 5 H), 1.81 (m, 1 H), 1.91–2.10 (m, 3 H), 2.12–2.28 (m, 3 H), 2.36 (m, 2 H), 2.47 (m, 2 H), 2.73 (m, 1 H), 4.43 (m, 2 H), 6.12 (m, 1 H), 7.35 (m, 1 H), 7.45 (m, 2 H), 7.61–7.69 (m, 4 H), 7.77 (s, 1 H), 7.91 (m, 2 H). ¹³C NMR (90 MHz, CDCl₃) δ 11.82, 21.15, 25.03, 25.95, 28.24, 28.40, 30.29, 49.53, 50.43, 52.39, 55.23, 94.50, 106.53, 119.33, 120.64, 126.08, 126.98, 127.41, 127.51, 128.81, 129.72, 135.28, 140.64, 140.85, 147.47. EIMS *m/z* 510. Anal. (C₃₂H₄₂N₄Si) C, H, N.

***N*-[4-[4-(4-Biphenyl)triazol-1-yl]butyl]-*N*-propyl-*N*-[4-(2-phenylethynyl)cyclohex-3-en-1-yl]amine (**5b**).** Compound **5b** was prepared according to the protocol of **10a** using a solution of **13** (11.4 mg, 0.02 mmol) in THF (5 mL), Cu(I)I (7.8 mg, 0.04 mmol), and Pd(PPh₃)₂Cl₂ (12.2 mg, 0.02 mmol) as well as NMe₂Et (0.05 mL, 0.46 mmol) and phenylacetylene (10 μL, 0.09 mmol). Stirring at room temperature for 90 min, workup according to **10a**, and purification by HPLC (CH₃CN–H₂O + 0.1% TFA) yielded **5b** as a white solid (TFA salt, 5.8 mg, 14% yield). IR: 3409, 2924, 2852, 1683, 1483, 1441, 1200, 1136, 1034, 845, 802, 765, 726, 692 cm⁻¹. ¹H NMR (360 MHz, CD₃OD/CHCl₃ 1:1, TFA salt) δ 1.04 (t, 3 H, *J* = 7.3 Hz), 1.69–1.87 (m, 5 H), 2.06–2.20 (m, 3 H), 2.38–2.62 (m, 4 H), 3.01–3.21 (m, 4 H), 3.52 (m, 1 H), 4.59 (m, 2 H), 6.08 (m, 1 H), 7.29–7.41 (m, 6 H), 7.45 (m, 2 H), 7.61–7.73 (m, 4 H), 7.90 (m, 2 H), 8.25 (s, 1 H). ¹³C NMR (90 MHz, CD₃OD/CHCl₃ 1:1, TFA salt) δ 11.25, 19.30 (HSQC), 22.73 (HSQC), 23.99, 26.83, 27.74, 29.66, 50.00, 50.97 (HSQC), 53.46 (HSQC), 59.92, 89.23, 121.80, 122.00, 123.76, 126.75, 127.53, 128.25, 129.03, 129.53, 129.85, 132.08, 141.18, 142.16, 148.61. HR-EIMS *m/z* 514.3096; purity HPLC.

***N*-[4-[4-(4-Biphenyl)triazol-1-yl]butyl]-*N*-propyl-*N*-(4-ethynylcyclohex-3-en-1-yl)amine (**5c**).** Compound **5c** was prepared according to the procedure of **4c** using a solution of **5a** (13.4 mg; 0.03 mmol) in THF (5 mL) and a 1 molar solution of tetrabutylammoniumfluoride (0.05 mL, 0.05 mmol). Stirring at –15 °C for 150 min, workup according to **4c**, and purification by flash chromatography (CH₂Cl₂–MeOH 98:2) and HPLC (CH₃CN–H₂O + 0.1% TFA) yielded **5c** as a white solid (TFA salt, 6.2 mg, 43% yield). IR: 3433, 3290, 2966, 2941, 2652, 2513, 1682, 1481, 1462, 1437, 1412, 1200, 1130, 831, 768 cm⁻¹. ¹H NMR (360 MHz, CD₃OD, TFA salt) δ 1.01 (t, 3 H, *J* = 7.4 Hz), 1.67–1.88 (m, 5 H), 2.03–2.15 (m, 3 H), 2.34–2.58 (m, 4 H), 3.00–3.24 (m, 4 H), 3.26 (s, 1 H), 3.56

(m, 1 H), 4.57 (m, 2 H), 6.06 (m, 1 H), 7.35 (m, 1 H), 7.45 (m, 2 H), 7.63–7.74 (m, 4 H), 7.90 (m, 2 H), 8.39 (s, 1 H). ¹³C NMR (150 MHz, CD₃OD, TFA salt) δ 11.18, 19.52, 19.73, 23.06, 23.26, 24.09, 26.96, 28.14, 29.82, 50.43, 51.34, 51.63, 53.72, 54.05, 60.47, 78.07, 84.19, 121.74, 122.43, 127.11, 127.86, 128.55, 128.65, 129.97, 130.56, 131.61, 141.70, 142.55, 148.88. HR-EIMS *m/z* 438.2783; purity HPLC.

4-Propylaminocyclohexan-1-one Ethylene Acetal (6). To a suspension of NaBH(OAc)₃ (2.13 g, 10.06 mmol) in THF (25 mL), a solution of 1,4-diazaspiro[4.5]decane-8-one (564.6 mg, 3.62 mmol), propylamine (0.33 mL, 4.01 mmol), and HOAc (0.23 mL, 4.01 mmol) in THF (15 mL) was added slowly at –10 °C. The flask of the solution was rinsed with THF (5 mL). The mixture was allowed to warm to room temperature. After being stirred at this temperature for 15 h, aqueous NaOH (10%) was added and the aqueous layer was extracted with CH₂Cl₂. The combined organic layers were washed with saturated aqueous NaCl and dried (MgSO₄). To this mixture, a solution of oxalic acid (686.8 mg) in MeOH (50 mL) was added at 0 °C and stirred at this temperature for 25 min. Then saturated aqueous NaHCO₃ was added, the mixture was stirred until no additional gas was formed, and the aqueous layer was extracted with CH₂Cl₂. The combined organic layers were dried (MgSO₄) and evaporated to give the crude **6** as a yellowish liquid (669.0 mg, 93% yield): analytical data according to the literature²¹

4-Azidobutanol Methane Sulfonate (7). After 4-chlorobutanol (7.5 mL, 75.16 mmol) was added to a suspension of NaN₃ (14.71 g, 226.35 mmol) and NaI (11.83 g, 78.93 mmol) in CH₃CN (225 mL) and H₂O (25 mL), the mixture was refluxed for 40 h. The mixture was cooled to room temperature, diluted with Et₂O, dried (MgSO₄), and evaporated to give crude 4-azidobutanol as an orange liquid (crude: 6.58 g, 75% yield).

To a solution of 4-azidobutanol (2.88 g, 24.56 mmol) in THF (40 mL), Et₃N (4.8 mL, 34.53 mmol) was added. After cooling the mixture to 0 °C and dropwise addition of methane sulfonylchloride (2.8 mL, 36.18 mmol), the reaction mixture was stirred at room temperature for 5.25 h. Then, a mixture of H₂O and ice (100 mL) was added and stirred until the ice was melted. The aqueous layer was separated and extracted with Et₂O. The combined organic layers were washed once with H₂O, once with aqueous 2N-HCl, once with H₂O, twice with saturated aqueous NaHCO₃, and once with H₂O, dried (MgSO₄), and evaporated to give the crude **7** as a red liquid (3.88 g, 81% yield).

4-[N-(4-Azidobutyl)-N-propyl]aminocyclohexan-1-one (8). To a suspension of **6** (2.51 g, 12.60 mmol), K₂CO₃ (8.89 g, 64.29 mmol) and NaI (4.07 g, 27.13 mmol) in CH₃CN (140 mL), a solution of **7** (6.41 g, 32.85 mmol) in CH₃CN (60 mL) was added. After being refluxed for 3 d, the mixture was cooled to room temperature and evaporated. The residue was dissolved in H₂O, basified with 6N NaOH, and the suspension was extracted with CH₂Cl₂. The combined organic layers were dried (MgSO₄) and evaporated. After dissolving the residue in acetone (80 mL), 6N HCl (150 mL) was added. After being stirred at room temperature for 19.5 h, 6N NaOH was added to basify the mixture. The aqueous layer was extracted with CH₂Cl₂. The combined organic layers were dried (MgSO₄) and evaporated. The residue was purified by flash chromatography (hexane–EtOAc 20:1 + 0.5% NMe₂Et) to give **8** as a colorless to slightly yellowish liquid (689.9 mg, 22% yield). IR (film): 3363, 2954, 2870, 2811, 2094, 1716, 1462, 1254, 1072, 949 cm^{–1}. ¹H NMR (600 MHz, CDCl₃) δ 0.88 (t, 3 H, *J* = 7.4 Hz), 1.44 (m, 2 H), 1.51 (m, 2 H), 1.59–1.66 (m, 2 H), 1.67–1.75 (m, 2 H), 2.02 (m, 2 H), 2.31–2.38 (m, 2 H), 2.39–2.46 (m, 4 H), 2.48 (m, 2 H), 2.95 (m, 1 H), 3.29 (m, 2 H). ¹³C NMR (150 MHz, CDCl₃) δ 11.75, 21.98, 25.99, 26.69, 27.93, 39.97, 50.01, 51.45, 52.51, 57.46, 211.29. EIMS *m/z* 252. Anal. (C₁₃H₂₄N₄O) C, H, N.

4-[N-(4-Azidobutyl)-N-propyl]aminocyclohex-1-en-1-yl Trifluoromethane Sulfonate (9). A solution of **8** (614.9 mg, 2.44 mmol) in 1,2-dichloroethane (40 mL) was added to 2,6-di-*tert*-butyl-4-methylpyridine (1032.8 mg, 5.03 mmol). Then, Tf₂O (0.85 mL, 5.12 mmol) was added slowly. After being refluxed for 4.5 h, the mixture was cooled to room temperature and aqueous NaHCO₃ was

added. The aqueous layer was extracted with CH₂Cl₂ and the combined organic layers were dried (MgSO₄) and evaporated. The residue was purified by flash chromatography (hexane–EtOAc 20:1 + 0.5% NMe₂Et) to give **9** as a yellowish oil (186.9 mg, 20% yield). IR: 3377, 2932, 2873, 2096, 1417, 1247, 1209, 1143, 1054, 1024, 873 cm^{–1}. ¹H NMR (600 MHz, CDCl₃) δ 0.87 (t, 3 H, *J* = 7.4 Hz), 1.38–1.52 (m, 4 H), 1.56–1.68 (m, 3 H), 1.82 (m, 1 H), 2.10–2.26 (m, 2 H), 2.34–2.51 (m, 6 H), 2.81 (m, 1 H), 3.28 (m, 2 H), 5.72 (m, 1 H). ¹³C NMR (150 MHz, CDCl₃) δ 11.75, 22.22, 24.83, 25.83, 26.22, 26.67, 28.01, 49.95, 51.46, 52.43, 57.73, 117.76, 118.51 (quart, *J* = 320.3 Hz), 148.41. HR-EIMS *m/z* 384.1444; purity HPLC.

N-(4-Azidobutyl)-N-propyl-N-[4-(2-trimethylsilylethynyl)cyclohex-3-en-1-yl]amine (10a). A solution of **9** (158.5 mg, 0.41 mmol) in THF (20 mL) was added to Cu(I)I (14.5 mg, 0.08 mmol) and Pd(PPh₃)₂Cl₂ (15.0 mg, 0.02 mmol). After addition of NMe₂Et (0.45 mL, 4.15 mmol) and TMS-acetylene (0.15 mL, 1.05 mmol), the mixture was stirred at room temperature for 40 min. Then, saturated aqueous NaHCO₃ was added, and the aqueous layer was extracted with Et₂O. The combined organic layers were dried (MgSO₄) and evaporated. The residue was purified by flash chromatography (hexane–EtOAc 40:1 + 0.5% NMe₂Et) to give **10a** as a yellowish oil (99.0 mg, 72% yield). IR: 3388, 2953, 2928, 2870, 2146, 2095, 1438, 1249, 1222, 1075, 1044, 860, 842, 772 cm^{–1}. ¹H NMR (600 MHz, CDCl₃) δ 0.17 (m, 9 H), 0.86 (t, 3 H, *J* = 7.4 Hz), 1.37–1.50 (m, 4 H), 1.57–1.64 (m, 3 H), 1.82 (m, 1 H), 2.00–2.08 (m, 1 H), 2.14–2.31 (m, 3 H), 2.37 (m, 2 H), 2.44 (m, 2 H), 2.74 (m, 1 H), 3.27 (m, 2 H), 6.13 (m, 1 H). ¹³C NMR (150 MHz, CDCl₃) δ 0.05, 11.83, 22.16, 25.06, 26.15, 26.75, 28.43, 30.29, 49.80, 51.50, 52.37, 55.23, 91.43, 106.57, 120.572, 135.44. HR-EIMS *m/z* 332.2398; purity HPLC.

N-(4-Azidobutyl)-N-propyl-N-[4-(2-phenylethynyl)cyclohex-3-en-1-yl]amine (10b). Compound **10b** was prepared according to the protocol of **10a** using a solution of **9** (194.3 mg, 0.51 mmol) in THF (10 mL) as well as Cu(I)I (11.6 mg, 0.06 mmol), Pd(PPh₃)₂Cl₂ (20.6 mg, 0.03 mmol), NMe₂Et (0.55 mL, 5.08 mmol), and phenylacetylene (0.11 mL, 1.0 mmol). Stirring at room temperature for 35 min, workup according to **10a**, and purification by flash chromatography (CH₂Cl₂–MeOH 100:0 to 98:2) gave crude **10b**, which was subsequently used for the next reaction step.

N-[4-(4-Methyltriazol-1-yl)butyl]-N-propyl-N-(4-propyn-1-yl)cyclohex-3-en-1-ylamine (11). A solution of **9** (333.7 mg, 0.87 mmol) in THF (3 mL) was added to Cu(I)I (28.6 mg, 0.15 mmol) and Pd(PPh₃)₂Cl₂ (63.0 mg, 0.09 mmol) in a pressure vial. After addition of piperidine (0.45 mL, 4.56 mmol), the mixture was cooled to –45 °C and propyne was bubbled through the solution for 20 min. After having sealed the vial, the mixture was stirred for 2 h at room temperature. Then, saturated aqueous NaHCO₃ was added and the aqueous layer was extracted with EtOAc. The combined organic layers were dried (MgSO₄) and evaporated. The residue was purified by HPLC (CH₃CN–H₂O + 0.1% TFA, gradient) to give **11** as a yellowish and soft solid (95.6 mg, 35% yield). IR: 2927, 2866, 1554, 1454, 1433, 1373, 1336, 1213, 1049, 640 cm^{–1}. ¹H NMR (360 MHz, CDCl₃) δ 0.84 (t, 3 H, *J* = 7.4 Hz), 1.33–1.49 (m, 5 H), 1.78 (m, 1 H), 1.85–1.95 (m, 5 H), 1.95–2.25 (m, 4 H), 2.31–2.39 (m, 5 H), 2.44 (m, 2 H), 2.72 (m, 1 H), 4.31 (m, 2 H), 5.94 (m, 1 H), 7.24 (s, 1 H). ¹³C NMR (150 MHz, CDCl₃) δ 4.12, 10.82, 11.81, 22.09, 25.10, 25.87, 28.21, 29.69, 30.64, 49.53, 50.08, 52.36, 55.32, 80.79, 83.28, 120.84, 120.88, 132.18, 143.27. EIMS *m/z* 314. Anal. (C₁₉H₃₀N₄) C, H, N.

4-[N-[4-(4-Biphenyl)triazol-1-yl]butyl]-N-propylaminocyclohexan-1-one (12). A suspension of **8** (766.5 mg, 3.04 mmol), 4-biphenylacetylene (1085.0 mg, 6.09 mmol), and [Cu(CH₃CN)₄]PF₆ (115.4 mg, 0.31 mmol) in CH₂Cl₂ (60 mL) and MeOH (20 mL) was stirred at 40 °C for 17 h. After further addition of 4-biphenylacetylene (1106.6 mg, 6.21 mmol) and [Cu(CH₃CN)₄]PF₆ (140.8 mg, 0.38 mmol), the mixture was stirred for another 8.5 h at 40 °C. Then, the solution was cooled to room temperature and evaporated. The residue was purified by flash chromatography (EtOAc + 0.5% NMe₂Et and CH₂Cl₂–MeOH 98:2 to 95:5) to give **12** as a white to yellowish solid (995.7 mg, 76% yield): mp 73 °C.

IR: 2804, 2744, 2318, 2285, 2256, 1641, 1390, 1022, 808, 733 cm^{-1} . ^1H NMR (360 MHz, CDCl_3) δ 0.86 (t, 3 H, $J = 7.4$ Hz), 1.36–1.55 (m, 4 H), 1.69 (m, 2 H), 1.95–2.05 (m, 4 H), 2.26–2.46 (m, 6 H), 2.50 (m, 2 H), 2.92 (m, 1 H), 4.44 (m, 2 H), 7.35 (m, 1 H), 7.45 (m, 2 H), 7.60–7.69 (m, 4 H), 7.78 (s, 1 H), 7.88–7.93 (m, 2 H). ^{13}C NMR (150 MHz, CDCl_3) δ 11.76, 21.99, 25.69, 27.85, 28.16, 39.97, 49.75, 50.35, 52.45, 57.42, 119.32, 126.02, 126.94, 127.42, 127.49, 128.79, 129.62, 140.54, 140.85, 147.483, 211.16. HR-EIMS m/z 430.2733; purity HPLC.

4-[[N-[4-[4-(4-Biphenyl)triazol-1-yl]butyl]-N-propyl]aminocyclohex-1-en-1-yl] Trifluoromethane Sulfonate (13). Compound **13** was prepared according to **9** using a solution of **12** (556.0 mg, 1.29 mmol) in 1,2-dichloroethane (20 mL), 2,6-di-*tert*-butyl-4-methylpyridine (820.5 mg, 4.00 mmol), and TiF_4 (0.65 mL, 3.92 mmol). Refluxing for 15 h, workup according to **9**, and rough purification by flash chromatography (hexane–EtOAc 1:1 + 0.5% NMe_2Et) gave crude **13**.

4-[[4-(4-Biphenyl)carbonyl]amino]butyl Methane Sulfonate (15). To a suspension of *N*-(4-hydroxybutyl)-4-biphenylcarboxamide (**14**, 1.34 g, 4.98 mmol) in THF (40 mL), Et_3N (1.0 mL, 7.19 mmol) was added. After cooling the mixture to 0 °C and dropwise addition of methane sulfonylchloride (0.6 mL, 7.75 mmol), the reaction mixture was stirred at room temperature for 2.5 h. Then, further methane sulfonylchloride (0.6 mL, 7.75 mmol) was added and the mixture was stirred overnight at room temperature. A mixture of H_2O and ice (50 mL) was added and stirred until the ice was melted. The aqueous layer was separated and extracted with CH_2Cl_2 . The combined organic layers were dried (MgSO_4) and evaporated to give crude **15**. A small sample of the residue was purified by flash chromatography with an SP-1 purification system (Biotage; hexane–EtOAc gradient) to give the analytical data: mp 133 °C. IR: 3314, 2941, 2861, 1632, 1539, 1449, 1432, 1347, 1168, 978, 938, 852, 831, 749 cm^{-1} . ^1H NMR (360 MHz, CDCl_3) δ 1.74–1.93 (m, 4 H), 3.03 (s, 3 H), 3.54 (m, 2 H), 4.31 (m, 2 H), 6.33 (m, 1 H), 7.39 (m, 1 H), 7.47 (m, 2 H), 7.59–7.69 (m, 4 H), 7.85 (m, 2 H). ^{13}C NMR (90 MHz, CDCl_3) δ 25.95, 26.59, 37.43, 39.18, 69.60, 127.17, 127.24, 127.36, 128.00, 128.91, 133.04, 139.94, 144.33, 167.34. HR-EIMS m/z 347.1191; purity HPLC.

***N*-(4-Propylaminobutyl)-4-biphenylcarboxamide (16a).** To a suspension of **15** (227.8 mg, 0.66 mmol), NaI (110.2 mg, 0.74 mmol), and K_2CO_3 (252.4 mg, 1.83 mmol) in CH_3CN (20 mL) and propylamine (0.15 mL, 1.82 mmol) were added. After being refluxed for 6 h, the mixture was cooled to room temperature and evaporated. The residue was dissolved with H_2O , basified with 2N NaOH, and extracted with CH_2Cl_2 . The combined organic layers were dried (MgSO_4) and evaporated. The residue was purified by HPLC ($\text{CH}_3\text{CN}/\text{H}_2\text{O}$ + 0.1% TFA, gradient) to give **16a** as a white solid (112.9 mg, 55% yield): mp 124 °C. IR: 3332, 2958, 2929, 2871, 2810, 1633, 1543, 1485, 1448, 1307, 1124, 851, 744, 689 cm^{-1} . ^1H NMR (360 MHz, CDCl_3) δ 0.91 (t, 3 H, $J = 7.4$ Hz), 1.45–1.78 (m, 6 H), 2.58 (m, 2 H), 2.69 (m, 2 H), 3.45 (m, 2 H), 7.18 (m, 1 H), 7.38 (m, 1 H), 7.46 (m, 2 H), 7.58–7.66 (m, 4 H), 7.84 (m, 2 H). ^{13}C NMR (90 MHz, CDCl_3) δ 11.41, 23.04, 27.46, 27.77, 40.00, 49.32, 51.89, 127.11, 127.19, 127.45, 127.89, 128.88, 133.69, 140.15, 144.01, 167.25. HR-EIMS m/z 310.2046; purity HPLC.

***N*-(4-Dipropylaminobutyl)-4-biphenylcarboxamide (16b).** Compound **16b** was prepared according to the procedure of **16a** using a suspension of **15** (265.9 mg, 0.77 mmol), NaI (186.6 mg, 1.24 mmol), and K_2CO_3 (258.9 mg, 1.87 mmol) in CH_3CN (20 mL) as well as dipropylamine (0.30 mL, 2.19 mmol). Refluxing for 16 h, workup according to **16a**, and purification by flash chromatography with an SP-1 purification system (Biotage; $\text{CH}_2\text{Cl}_2/\text{MeOH}$, gradient) gave **16b** as a white and soft solid (145.0 mg, 53% yield). IR: 3416, 3320, 3057, 3033, 2959, 2937, 2874, 2795, 1633, 1547, 1486, 1308, 1160, 856, 748, 697 cm^{-1} . ^1H NMR (360 MHz, CDCl_3) δ 0.94 (t, 6 H, $J = 7.4$ Hz), 1.63–1.90 (m, 8 H), 2.77 (m, 4 H), 2.86 (m, 2 H), 3.54 (m, 2 H), 7.37 (m, 1 H), 7.45 (m, 2 H), 7.59–7.68 (m, 4 H), 8.00 (m, 2 H). ^{13}C (90 MHz, CDCl_3) δ 11.41, 17.67, 22.31,

26.59, 38.62, 52.78, 54.58, 127.07, 127.15, 127.74, 127.83, 128.84, 133.04, 140.13, 144.01, 167.36. HR-EIMS m/z 352.2515; purity HPLC.

***N*-[(*N'*-(4-Cyclohexyl)-*N'*-propyl)aminobutyl]-4-biphenylcarboxamide (16c).** *N*-[(*N'*-Cyclohexyl)-4-aminobutyl]-4-biphenylcarboxamide was prepared according to the procedure of **16a** using a suspension of **15** (492.5 mg, 1.42 mmol), NaI (228.2 mg, 1.52 mmol), and K_2CO_3 (410.1 mg, 2.97 mmol) in CH_3CN (20 mL) as well as cyclohexylamine (0.50 mL, 4.37 mmol). Refluxing for 14 h, workup according to **16a**, and purification by flash chromatography with an SP-1 purification system (Biotage; $\text{CH}_2\text{Cl}_2/\text{MeOH}$, gradient) gave the intermediate as a white to yellowish solid (245.8 mg, 49% yield): mp 103 °C. IR: 3316, 2925, 2852, 2807, 1633, 1582, 1447, 1309, 1126, 853, 746 cm^{-1} . ^1H NMR (600 MHz, $\text{CDCl}_3/\text{CD}_3\text{OD}$) δ 1.05 (m, 2 H), 1.14 (m, 1 H), 1.25 (m, 2 H), 1.53–1.70 (m, 5 H), 1.74 (m, 2 H), 1.89 (m, 2 H), 2.42 (m, 1 H), 2.65 (m, 2 H), 3.45 (m, 2 H), 7.38 (m, 1 H), 7.46 (m, 2 H), 7.59–7.68 (m, 4 H), 7.88 (m, 2 H). ^{13}C NMR (150 MHz, $\text{CDCl}_3/\text{CD}_3\text{OD}$) δ 24.85, 25.78, 26.85, 27.09, 32.86, 39.55, 45.86, 56.70, 126.89, 126.97, 127.42, 127.76, 128.71, 133.05, 139.89, 143.98, 167.96. EIMS m/z 350; purity HPLC.

To a suspension of *N*-[(*N'*-cyclohexyl)-4-aminobutyl]-4-biphenylcarboxamide (117.8 mg, 0.34 mmol) and $\text{NaBH}(\text{OAc})_3$ (160.5 mg, 0.76 mmol) in CH_2Cl_2 (20 mL), propionaldehyde (0.05 mL, 0.67 mmol) was added. After being stirred at room temperature for 7 h, the solution was evaporated. The residue was dissolved in concentrated HCl and washed with Et_2O . The aqueous layer was basified with 2N NaOH and extracted with Et_2O . The combined organic layers were dried (MgSO_4) and evaporated. The residue was purified by HPLC ($\text{CH}_3\text{CN}/\text{H}_2\text{O}$ + 0.1% TFA, gradient) to give **16c** as a white solid (112.9 mg, 55% yield): mp 87 °C. IR: 3323, 2928, 2854, 2802, 1634, 1542, 1448, 1307, 1074, 852, 745 cm^{-1} . ^1H NMR (360 MHz, CDCl_3) δ 0.85 (t, 3 H, $J = 7.3$ Hz), 1.14–1.28 (m, 5 H), 1.40–1.85 (m, 11 H), 2.46 (m, 2 H), 2.50–2.61 (m, 3 H), 3.50 (m, 2 H), 6.78 (m, 1 H), 7.38 (m, 1 H), 7.46 (m, 2 H), 7.59–7.67 (m, 4 H), 7.86 (m, 2 H). C (90 MHz, CDCl_3) δ 11.89, 21.57, 26.12, 26.27, 27.37, 28.64, 39.86, 50.11, 52.69, 60.34, 127.14, 127.19, 127.47, 127.89, 128.88, 133.59, 140.14, 144.03, 167.32. HR-EIMS m/z 392.2832; purity HPLC.

Dopamine Receptor Binding Studies. Receptor binding studies were carried out as described.⁹ In brief, the dopamine D_1 receptor assay was done with porcine striatal membranes at a final protein concentration of 40 $\mu\text{g}/\text{assay tube}$ and the radioligand [^3H]SCH 23390 at 0.3 nM ($K_D = 0.41\text{--}0.58$ nM). Competition experiments with human $\text{D}_{2\text{long}}$,²⁴ $\text{D}_{2\text{short}}$,²⁴ D_3 ,²⁵ and $\text{D}_{4.4}$ ²⁶ receptors were run with preparations of membranes from CHO cells stably expressing the corresponding receptor and [^3H]spiperone at a final concentration of 0.1–0.2 nM. The assays were carried out at a protein concentration of 5–20 $\mu\text{g}/\text{assay tube}$ and K_D values of 0.07–0.15, 0.05–0.13, 0.11–0.19, and 0.17–0.35 nM for the $\text{D}_{2\text{long}}$, $\text{D}_{2\text{short}}$, D_3 , and $\text{D}_{4.4}$ receptors, respectively. 5-HT and α_1 receptor binding experiments were performed with homogenates prepared from porcine cerebral cortex as described.⁴⁰ Assays were run with membranes at a protein concentration per each assay tube of 100, 80, and 60 $\mu\text{g}/\text{mL}$ for 5-HT $_{1A}$, 5-HT $_2$, and α_1 receptor, respectively, and radioligand concentrations of 0.1 nM ([^3H]WAY100635 and [^3H]prazosin) and 0.5 nM ([^3H]ketanserin) with K_D values of 0.3–0.11 nM for 5-HT $_{1A}$, 1.5–2.7 nM for 5-HT $_2$, and 0.06–0.09 nM for the α_1 receptor. Protein concentration was established by the method of Lowry using bovine serum albumin as standard.⁴¹

Data Analysis. The resulting competition curves of the receptor binding experiments were analyzed by nonlinear regression using the algorithms in PRISM 3.0 (GraphPad Software, San Diego, CA). The data were initially fit using a sigmoid model to provide an IC_{50} value, representing the concentration corresponding to 50% of maximal inhibition. For more detailed analysis, data of selected compounds was calculated for a one-site ($n_H \sim 1$) or a two-site model ($n_H < 1$) depending on the slope factor. IC_{50} values were transformed to K_i or $K_{0.5}$ values as well as to K_i^{high} and K_i^{low} in

the fact when a two-site model was preferred after fitting mono- and biphasic curves according to the equation of Cheng and Prusoff.⁴²

Mitogenesis Experiments. Determination of the ligand efficacy of representative compounds was carried out by measuring the incorporation of [³H]thymidine into growing cells after stimulation with the test compound as described in the literature.^{43,44} For this assay D₃ expressing CHO dhfr⁻ cells have been incubated with 0.02 μ Ci [³H]thymidine per well (specific activity 25 μ Ci/mmol). Dose response curves of 6–10 experiments have been normalized and summarized to get a mean curve from which the EC₅₀ value, and the maximum intrinsic activity of each compound could be compared to the effects of the full agonist quinpirole.

cAMP Assay. Bioluminescence based cAMP-Glo assay (Promega) was performed according to the manufacturers instructions. Briefly, CHO cells expressing D₃ receptor were seeded into a white 96-well plate (5000 cells/well) 24 h before the assay. On the day of the assay, cells were briefly washed with Krebs–Ringer Buffer to remove traces of serum and were incubated with various concentrations of substances in the presence of 20 μ M forskolin in Krebs–Ringer buffer that contained 100 μ M IBMX and 100 μ M Ro 20-1724. After 15 min of incubation at room temperature, cells were lysed using cAMP-Glo lysis buffer. After lysis, the kinase reaction was performed using reaction buffer containing PKA. At the end of the kinase reaction, an equal volume of Kinase-Glo reagent was added. The plates were read using a luminescence protocol on microplate reader Victor 3 (Perkin-Elmer).

Cloning, Site Directed Mutagenesis, and Transfection. The cDNA of human dopamine 3 receptor (D₃) chimera was a kind gift of Dr. Roberto Maggio (University of L'Aquila). The mutation within intracellular loop 3 was reversed by overlap PCR. The overlapping regions of the DRD3 were amplified using two flanking nucleotides, forward 5'-TAATACGACTCACTATAGGG-3' and reverse 5'-ACTAGAAGGCAGTCGAGG-3', in combination with overlapping nucleotides containing mutated sequence (forward 5'-CTGCAACCTCGGGGAGTGCCACTTCGGGA-GAAGAAGGCAACC-3', reverse 5'-GCACTCCCCGAGGTTG-CAGGGGCCCCAGCTTCAAAGATGTCG-3'). The construct was cloned into pcDNA5 vector (Invitrogen) after restriction digestion with HindIII/XbaI. The sequence of the new construct was confirmed by sequencing reaction. This cDNA of the D₃ receptor was then used for site directed mutagenesis by overlap PCR. The overlapping regions of the D₃ were amplified using two the same flanking nucleotides as above. The overlapping nucleotides contained mutated residues D3.32E (forward 5'-ATGTTTTTGTCCACCTCGAGGTCATGATG-3', reverse 5'-CACATCATGACCTCGAGGTTGACAAAACAT-3') or F6.51W (forward 5'-CTGCTGGTTGCCGGCATTCTTGAC-3', reverse 5'-GTCAAGAACAGGGTAACCAGCAGAC-3'). The final PCR product was digested with BamHI/HindIII for D₃ D3.32E and BamHI/BstEII for D₃ F6.51W, cloned into D₃ wild type vector, and sequenced to ensure that correct mutations were introduced.

The 293 human embryonic kidney (293 HEK) cells were transfected using either TransIT-293 transfection reagent (Mirus Bio Corporation) or calcium phosphate precipitation method.⁴⁵ The 293 HEK cell line was maintained in α -MEM supplemented with 10% FBS, 2 mM L-glutamine, and 1% Pen-Strep, and cultured at 37 °C in 5% CO₂. Forty-eight hours after transfection, cells were harvested and processed as described previously.⁹

Binding Assays for Mutants. Competition binding assays with D₃ wild type, D₃ D3.32E, and D₃ F6.51W mutant receptors were performed on membrane preparations from HEK cells transiently expressing corresponding receptor and [³H]spiperone at the final concentrations of 0.1–0.6 nM, as described above. The assays were carried out in the 96-well plates at the protein concentration of 20–200 μ g/mL in the final volume of 200 μ L. The K_D values were 0.52 \pm 0.10, 1.85 \pm 0.24, and 0.23 \pm 0.08 nM for the D₃, D₃ D3.32E, and D₃ F6.51W receptors, respectively.

Acknowledgment. We thank Dr. H. H. M. Van Tol (Clarke Institute of Psychiatry, Toronto, Canada), Dr. J.-C. Schwartz,

Dr. P. Sokoloff (INSERM, Paris), and Dr. J. Shine (The Garvan Institute of Medical Research, Sydney) for providing dopamine D₄, D₃, and D₂ receptor expressing cell lines, respectively, and Dr. R. Maggio (University of L'Aquila) for providing the cDNA of a human D₃ receptor chimera.

Supporting Information Available: NMR spectra, combustion analysis data, HPLC purity data including spectra and HR-EIMS analysis data. This material is available free of charge via the Internet at <http://pubs.acs.org>.

References

- (1) Neve, K. A.; Neve, R. L. *The Dopamine Receptors*, 1st ed.; Humana Press: Totowa, NJ, 1996.
- (2) Unis, A. S.; Roberson, M. D.; Hill, K.; Hamblin, M. W.; Dorsa, D. W. Differential localization of D₂ versus D₃ mRNA in midgestational human forebrain by in situ hybridization Society of Neuroscience Abstracts; Society of Neuroscience: Washington, DC, 1995, Vol. 21, p 1620.
- (3) Schmidt, N.; Ferger, B. Neurochemical findings in the MPTP model of Parkinson's disease. *J. Neural Transm.* **2001**, *108*, 1263–1282.
- (4) Boeckler, F.; Leng, A.; Mura, A.; Bettinetti, L.; Feldon, J.; Gmeiner, P.; Ferger, B. Attenuation of 1-methyl-4-phenyl-1,2,3,6-tetrahydropyridine (MPTP) neurotoxicity by the novel selective dopamine D₃-receptor partial agonist FAUC 329 predominantly in the nucleus accumbens of mice. *Biochem. Pharmacol.* **2003**, *66*, 1025–1032.
- (5) Boeckler, F.; Gmeiner, P. Dopamine D₃ receptor ligands—recent advances in the control of subtype selectivity and intrinsic activity. *Biochim. Biophys. Acta, Biomembr.* **2007**, *1768*, 871–887.
- (6) Boeckler, F.; Gmeiner, P. The structural evolution of dopamine D₃ receptor ligands: Structure–activity relationships and selected neuropharmacological aspects. *Pharmacol. Ther.* **2006**, *112*, 281–333.
- (7) Boyfield, I.; Coldwell, M. C.; Hadley, M. S.; Johnson, C. N.; Riley, G. J.; Scott, E. E.; Stacey, R.; Stemp, G.; Thewlis, K. M. A novel series of 2-aminotetralins with high affinity and selectivity for the dopamine D₃ receptor. *Bioorg. Med. Chem. Lett.* **1997**, *7*, 1995–1998.
- (8) van Vliet, L. A.; Tepper, P. G.; Dijkstra, D.; Damsma, G.; Wikström, H.; Pugsley, T. A.; Akunne, H. C.; Heffner, T. G.; Glase, S. A.; Wise, L. D. Affinity for Dopamine D₂, D₃, and D₄ Receptors of 2-Aminotetralins. Relevance of D₂ Agonist Binding for Determination of Receptor Subtype Selectivity. *J. Med. Chem.* **1996**, *39*, 4233–4237.
- (9) Hübner, H.; Haubmann, C.; Utz, W.; Gmeiner, P. Conjugated Enynes as Nonaromatic Catechol Bioisosteres: Synthesis, Binding Experiments, and Computational Studies of Novel Dopamine Receptor Agonists Recognizing Preferentially the D₃ Subtype. *J. Med. Chem.* **2000**, *43*, 756–762.
- (10) Lenz, C.; Boeckler, F.; Hübner, H.; Gmeiner, P. Analogues of FAUC 73 revealing new insights into the structural requirements of nonaromatic dopamine D₃ receptor agonists. *Bioorg. Med. Chem.* **2004**, *12*, 113–117.
- (11) Lenz, C.; Boeckler, F.; Hübner, H.; Gmeiner, P. Fancy bioisosteres: Synthesis, SAR, and pharmacological investigations of novel nonaromatic dopamine D₃ receptor ligands. *Bioorg. Med. Chem.* **2005**, *13*, 4434–4442.
- (12) Lenz, C.; Haubmann, C.; Hübner, H.; Boeckler, F.; Gmeiner, P. Fancy bioisosteres: synthesis and dopaminergic properties of the endiary FAUC 88 as a novel non-aromatic D₃ agonist. *Bioorg. Med. Chem.* **2005**, *13*, 185–191.
- (13) Bolton, D.; Boyfield, I.; Coldwell, M. C.; Hadley, M. S.; Healy, M. A. M.; Johnson, C. N.; Markwell, R. E.; Nash, D. J.; Riley, G. J.; Stemp, G.; Wadsworth, H. J. Novel 2,5-Disubstituted-1 H-Pyrroles with high affinity for the Dopamine D₃ Receptor. *Bioorg. Med. Chem. Lett.* **1996**, *6*, 1233–1236.
- (14) Micheli, F.; Bonanomi, G.; Blaney, F. E.; Braggio, S.; Capelli, A. M.; Checchia, A.; Curcuruto, O.; Damiani, F.; Di Fabio, R.; Donati, D.; Gentile, G.; Gribble, A.; Hamprecht, D.; Tedesco, G.; Terreni, S.; Tarsi, L.; Lightfoot, A.; Stemp, G.; MacDonald, G.; Smith, A.; Pecoraro, M.; Petrone, M.; Perini, O.; Piner, J.; Rossi, T.; Worby, A.; Pilla, M.; Valerio, E.; Griffante, C.; Mugnaini, M.; Wood, M.; Scott, C.; reoli, M.; Lacroix, L.; Schwarz, A.; Gozzi, A.; Bifone, A.; Ashby, J.; C. R.; Hagan, J. J.; Heidbreder, C. 1,2,4-Triazol-3-yl-thiopropyl-tetrahydrobenzazepines: A Series of Potent and Selective Dopamine D₃ Receptor Antagonists. *J. Med. Chem.* **2007**, *50*, 5076–5089.
- (15) Micheli, F.; Bonanomi, G.; Braggio, S.; Capelli, A. M.; Celestini, P.; Damiani, F.; Di Fabio, R.; Donati, D.; Gagliardi, S.; Gentile, G.; Hamprecht, D.; Petrone, M.; Radaelli, S.; Tedesco, G.; Terreni, S.; Worby, A.; Heidbreder, C. New fused benzazepine as selective D₃ receptor antagonists. Synthesis and biological evaluation. Part one: [h]-fused tricyclic systems. *Bioorg. Med. Chem. Lett.* **2008**, *18*, 901–907.

- (16) Micheli, F.; Bonanomi, G.; Braggio, S.; Capelli, A. M.; Damiani, F.; Di Fabio, R.; Donati, D.; Gentile, G.; Hamprecht, D.; Perini, O.; Petrone, M.; Tedesco, G.; Terreni, S.; Worby, A.; Heidbreder, C. New fused benzazepine as selective D₃ receptor antagonists. Synthesis and biological evaluation. Part 2: [g]-Fused and heterofused systems. *Bioorg. Med. Chem. Lett.* **2008**, *18*, 908–912.
- (17) Cha, M. Y.; Choi, B. C.; Kang, K. H.; Pae, A. N.; Choi, K. I.; Cho, Y. S.; Koh, H. Y.; Lee, H.-Y.; Jung, D.; Kong, J. Y. Design and Synthesis of a Piperazinylalkylisoxazole Library for Subtype Selective Dopamine Receptor Ligands. *Bioorg. Med. Chem. Lett.* **2002**, *12*, 1327–1330.
- (18) Bock, V. D.; Hiemstra, H.; van Maarseveen, J. H. Cu^I-Catalyzed Alkyne-Azide “Click” Cycloadditions from a Mechanistic and Synthetic Perspective. *Eur. J. Org. Chem.* **2006**, *5*, 1–68.
- (19) Paul, A.; Bittermann, H.; Gmeiner, P. Triazolepeptides: chiroselective synthesis and cis/trans prolyl ratios of structural isomers. *Tetrahedron* **2006**, *62*, 8919–8927.
- (20) Rodriguez Loaiza, P.; Löber, S.; Hübner, H.; Gmeiner, P. Click Chemistry on Solid Phase: Parallel Synthesis of *N*-Benzyltriazole Carboxamides as Super-Potent G-Protein Coupled Receptor Ligands. *J. Comb. Chem.* **2006**, *8*, 252–261.
- (21) Pascual Coca, G.; Martín Juárez J. Method of obtaining 2-amino-6-alkyl-amino-4,5,6,7-tetrahydrobenzothiazoles. Patent WO 2006/003220 A1, 2006.
- (22) Gomes Faraco, A. A.; Prado, M. A. F.; Alves, R. J.; Souza Filho, J. D.; Brondi Alves, R.; Prado Faraco, R. F. Synthesis of Benzomacrolactam by 12-endo Selective Aryl Radical Cyclization of *N*-(4-Allyloxybutyl)-2-iodobenzamide. *Synth. Commun.* **2003**, *33*, 463–474.
- (23) Stemp, G.; Johnson, C. N. Bicyclic amine derivatives and their use as antipsychotic agents. Patent WO 96/30333, 1996.
- (24) Hayes, G.; Biden, T. J.; Selbie, L. A.; Shine, J. Structural subtypes of the dopamine D₂ receptor are functionally distinct: expression of the cloned D_{2A} and D_{2B} subtypes in a heterologous cell line. *Mol. Endocrinol.* **1992**, *6*, 920–926.
- (25) Sokoloff, P.; Andrieux, M.; Besancon, R.; Pilon, C.; Martres, M.-P.; Giros, B.; Schwartz, J.-C. Pharmacology of human dopamine D₃ receptor expressed in a mammalian cell line: comparison with D₂ receptor. *Eur. J. Pharmacol.* **1992**, *225*, 331–337.
- (26) Asghari, V.; Senyal, S.; Buchwaldt, S.; Paterson, A.; Jovanovic, V.; Van Tol, H. H. M. Modulation of intracellular cyclic AMP levels by different human D₄ receptor variants. *J. Neurochem.* **1995**, *65*, 1157–1165.
- (27) Elsner, J.; Boeckler, F.; Heinemann, F. W.; Hübner, H.; Gmeiner, P. Pharmacophore-Guided Drug Discovery Investigations Leading to Bioactive 5-Aminotetrahydropyrazolopyridines. Implications for the Binding Mode of Heterocyclic Dopamine D₃ Receptor Agonists. *J. Med. Chem.* **2005**, *48*, 5771–5779.
- (28) Kumar, M.; Hsiao, K.; Vidugiriene, J.; Goueli, S. A. A Bioluminescent-Based, HTS-Compatible Assay to Monitor G-Protein-Coupled Receptor Modulation of Cellular Cyclic AMP. *Assay Drug Dev. Technol.* **2007**, *5*, 237–245.
- (29) Mailman, R. B. GPCR functional selectivity has therapeutic impact. *Trends Pharmacol. Sci.* **2007**, *28*, 390–396.
- (30) Gay, E. A.; Urban, J. D.; Nicols, D. E.; Oxford, G. S.; Mailman, R. B. Functional Selectivity of D₂ Receptor Ligands in a Chinese Hamster Ovary hD_{2L} Cell Line: Evidence for Induction of Ligand-Specific Receptor States. *Mol. Pharmacol.* **2004**, *66*, 97–105.
- (31) Lane, J. R.; Powey, B.; Wise, A.; Rees, S.; Milligan, G. G Protein Coupling and Ligand Selectivity of the D_{2L} and D₃ Dopamine Receptors. *J. Pharmacol. Exp. Ther.* **2008**, *325*, 319–330.
- (32) Ahlgren-Beckendorf, J. A.; Levant, B. Signaling Mechanisms of the D₃ Dopamine Receptor. *J. Recept. Signal Transduction* **2004**, *24*, 117–130.
- (33) Cho, D.-I.; Oak, M.-H.; Yange, H.-J.; Choi, H.-K.; Janssen, G. M. C.; Kim, K.-M. Direct and biochemical interaction between dopamine D₃ receptor and elongation factor-1Bγ. *Life Sci.* **2003**, *73*, 2991–3004.
- (34) Boeckler, F.; Ohnmacht, U.; Lehmann, T.; Utz, W.; Hübner, H.; Gmeiner, P. CoMFA and CoMSIA Investigations Revealing Novel Insights into the Binding Modes of Dopamine D₃ Receptor Agonists. *J. Med. Chem.* **2005**, *48*, 2493–2508.
- (35) Cho, W.; Taylor, L. P.; Mansour, A.; Akil, H. Hydrophobic residues of the D₂ dopamine receptor are important for binding and signal transduction. *J. Neurochem.* **1995**, *65*, 2105–2115.
- (36) Javitch, J. A.; Ballersteros, J. A.; Weinstein, H.; Chen, J. A cluster of aromatic residues in the sixth membrane-spanning segment of the dopamine D₂ receptor is accessible in the binding-site crevice. *Biochemistry* **1998**, *37*, 998–1006.
- (37) Miller, D. D.; Harrold, M.; Wallace, R. A.; J., W. L.; Uretsky, N. J. Dopaminergic drugs in the cationic form interact with D₂ dopamine receptors. *Trends Pharmacol. Sci.* **1988**, *9*, 282–284.
- (38) Bordo, D.; Argos, P. Suggestions for “safe” residue substitutions in site directed mutagenesis. *J. Mol. Biol.* **1991**, *217*, 721–729.
- (39) Borea, P. A.; Dalpiaz, A. D.; Varani, K.; Gilli, P.; Gilli, G. Can Thermodynamic Measurements of Receptor Binding Yield Information on Drug Affinity and Efficacy? *Biochem. Pharmacol.* **2000**, *60*, 1549–1556.
- (40) Heindl, C.; Hübner, H.; Gmeiner, P. Ex-chiral pool synthesis and receptor binding studies of 4-substituted prolinol derivatives. *Tetrahedron: Asymmetry* **2003**, *14*, 3141–3152.
- (41) Lowry, O. H.; Rosebrough, N. J.; Farr, A. L.; Randall, R. J. Protein measurement with the Folin phenol reagent. *J. Biol. Chem.* **1951**, *193*, 265–275.
- (42) Cheng, Y.; Prusoff, W. H. Relationship between the inhibition constant (K_i) and the concentration of inhibitor which causes 50% inhibition (I₅₀) of an enzymatic reaction. *Biochem. Pharmacol.* **1973**, *22*, 3099–3108.
- (43) Hübner, H.; Kraxner, J.; Gmeiner, P. Cyanoindole Derivatives as Highly Selective Dopamine D₄ Receptor Partial Agonists: Solid-Phase Synthesis, Binding Assays, and Functional Experiments. *J. Med. Chem.* **2000**, *43*, 4563–4569.
- (44) Bettinetti, L.; Schlotter, K.; Hübner, H.; Gmeiner, P. Interactive SAR Studies: Rational Discovery of Super-Potent and Highly Selective Dopamine D₃ Receptor Antagonists and Partial Agonists. *J. Med. Chem.* **2002**, *45*, 4594–4597.
- (45) Jordan, M.; Schallhorn, A.; Wurm, F. M. Transfecting mammalian cells: optimization of critical parameters affecting calcium-phosphate precipitate formation. *Nucleic Acids Res.* **1996**, *24*, 596–601.

JM800895V